RSC Advances

PAPER

View Article Online
View Journal | View Issue

Cite this: *RSC Adv.*, 2015, **5**, 92025

An electrochemical sensing strategy for the detection of the hepatitis B virus sequence with homogenous hybridization based on host–guest recognition†

Jing Zheng,*[ab] Liping Hu,[a] Min Zhang,[a] Jingli Xu[a] and Pingang He[b]

Rapid, sensitive, and accurate DNA detection is of great significance to meet the growing demand of disease diagnostics. Herein, an ultrasensitive and highly specific electrochemical sensing strategy for detection of hepatitis B virus (HBV) DNA hybridization in homogeneous solution was presented. In this sensing protocol, magnetic nanoparticles (MNPs) were prepared and modified with β-CD. MNPs/β-CD were then used for host–guest recognition, separation and detection. In the experiment, a stem-loop structured DNA was designed as the probe to indicate the occurrence of hybridization. It was labeled with dabcyl at the 5′-end as a guest molecule and Au nanoparticles at the 3′-end as an electrochemical tag. Initially, the DNA probe retained the stem-loop configuration, which shielded dabcyl from docking with β-CD/MNP in solution due to the steric effect. While in the presence of the complementary target DNA, the stem-loop structure of the probe was dissociated and the double-stranded DNA (dsDNA) was formed as a result of the hybridization. Consequently, dsDNA was linked to β-CD/MNP owing to the host–guest recognition between β-CD and dabcyl. Thus, the hybridization events could be sensitively transduced to electrochemical signals provided by Au nanoparticles. Au nanoparticles were then captured by the electrode through an external magnetic field. The designed sensor favored discrimination between the healthy and single-nucleotide polymorphism (SNP)-containing sequences. Under the optimized detection conditions, the sensing strategy showed high sensitivity and the detection limit was down to 9.930×10^{-13} M for a complementary HBV DNA sequence.

Received 16th August 2015
Accepted 18th October 2015

DOI: 10.1039/c5ra16204a

www.rsc.org/advances

1. Introduction

The sequence-specific detection of DNA has attracted considerable interest in numerous fields, such as medical diagnostics, gene expression analysis, environmental monitoring and identification of infectious diseases.[1–3] A variety of techniques are established for the detection of DNA sequences, such as fluorescence,[4] chemiluminescence,[5] electrochemistry[6] and surface plasmon resonance,[7] *etc.*

The electrochemical technology used for DNA detection has received particular attention mostly due to its high sensitivity, selectivity and easy operation with simple instrumentation.[8,9] Different electrochemical strategies have been explored for the detection of DNA, including intrinsic electroactivity of the nucleic acid,[10] DNA duplex intercalators,[11] electroactive markers,[12] enzyme labels[13] and metal nanoparticles/quantum dots tracers.[14] Among these strategies, electrochemical methods using nanoparticles have opened a new route for sensitive and selective detection.[15,16] Nanoparticles offered excellent prospects for DNA detection because of their unique physical and chemical properties.[17] Magnetic nanoparticles (MNPs) have been widely used in bioanalysis because they serve as both the solid support and the means of separation in the system. They can also collect the sample by magnetic field to offer promise as sensitive sensors.[18] Likewise, Au nanoparticles are excellent candidate for bioconjugation, owing to the fact that they are compatible. It can bind with a range of biomolecules such as amino acids, protein, enzymes and DNA.[19] While, the traditional electrochemical DNA detection methods mostly need probe DNA pre-immobilization on the electrode surface.[20–22] These methods might affect the immobilization efficiency, hybridization efficiency and detection sensitivity.[23] Therefore, exploring the non-immobilization approaches for the electrochemical DNA detection has received particular attention. In recent years, using non-immobilization techniques to realize DNA homogenous hybridization has been

[a]*Department of Chemistry & Chemical Engineering, Shanghai University of Engineering Science, Shanghai, 201620, P. R. China. E-mail: kkzhengjing707@163.com; Tel: +86 21 67791214*

[b]*Department of Chemistry, East China Normal University, Shanghai, 200062, P. R. China*

† Electronic supplementary information (ESI) available: The UV-vis spectra of probe DNA, the FT-IR spectra of MNPs/β-CD, energy-dispersive spectroscopy (EDS) spectrum and the TEM image of the conjugate of MNPs/β-CD–target DNA–probe DNA/Au conjugates. See DOI: 10.1039/c5ra16204a

reported. A non-immobilizing electrochemical DNA sensing strategy with homogenous hybridization has been reported by Han and co-workers.[24] One-step homogeneous detection of DNA hybridization by using a linear light-scattering technique has been presented by Du and co-workers.[25] Storhoff has also reported homogeneous detection of unamplified genomic DNA sequences based on colorimetric scatter of gold nanoparticle probes.[26]

The molecular recognition technology, defined as the supramolecular noncovalent interaction between the "host" and "guest" molecules, has been previously employed in the chemical sensing field.[27,28] Cyclodextrins (CDs) are one kind of special oligosaccharides, which consist of six, seven, or eight glucose units. Their exterior and cavity are respectively hydrophilic and hydrophobic, which enabled CDs as the host to accommodate the hydrophobic guest molecules with suitable dimensions into the cavity. The unique "cage" structure endows CDs and their derivatives with outstanding recognition and encapsulation abilities to their guest molecules. Consequently, they have been employed as the host molecule in electrochemistry.[29,30] Recently, the CDs modified electrodes as selective electrodes for sequence-specific DNA detection have attracted great interest. Yang and his co-workers have used the β-cyclodextrin functionalized electrode to detect the DNA hybridization based on the host–guest recognition technology.[31]

Since hepatitis B is a prevalent and potentially life-threatening disease caused by the hepatitis B virus (HBV),[32] about 350 million people worldwide are chronic carriers of HBV, and more than 620 000 die from liver-related diseases each year.[33] It is imperative to propose a highly sensitive and inexpensive protocol for detection of HBV. As far as we know, some methods for the detection of HBV have been reported including single strand conformation,[34] high performance liquid chromatography (HPLC),[35] the surface-enhanced Raman scattering detection,[36] polymerase chain reaction (PCR),[37–39] and restriction fragment length polymorphism (RFLP).[40] While the surface-enhanced Raman scattering is inefficient due to the small Raman scattering cross section of molecules. High performance liquid chromatography (HPLC), the polymerase chain reaction (PCR) and restriction fragment length polymorphism (RFLP) are complex, time-consuming and toxic. Therefore, it is urgent to develop a simple, rapid, sensitive and selective method for the detection of HBV. In this paper, a non-immobilizing electrochemical sensor based on the host–guest recognition for detecting HBV DNA sequence is developed.

In this paper, a specific electrochemical sensing strategy for detection of hepatitis B virus (HBV) DNA hybridization in homogeneous solution was presented. In this strategy, a special DNA probe with a stem-loop structure was designed to fulfill electrochemical DNA detection. The DNA probe, composed of a self-complementary stem and a loop. Its stem-loop structure was formed through the base pairing and the sequences in the loop were complementary to the target HBV specific sequence. The special hairpin-like DNA stem-loop structure has been reported to exhibit high differentiation ability toward single-nucleotide polymorphisms.[41] The probe was labeled with dabcyl molecules as guest at the 5′-end and Au nanoparticles as an electrochemical tag at the 3′-end. β-Cyclodextrin (β-CD) immobilized magnetic nanoparticle (MNPs/β-CD) was synthesized and used to detect DNA hybridization in the solution based on host–guest recognition technology. The CD/dabcyl host–guest complex served to be responsible for the specific recognition event used to detect the target. As shown in Fig. 1, in the absence of the target DNA sequence, the probe was in a stem-loop structure and would not be captured and detected by the electrode. Only in the presence of the complementary target sequence did the probe unfold and transform into a straight double-stranded DNA state. In this state, the dabcyl molecule was no longer in close contact with the Au nanoparticle, and consequently it could be captured by the MNPs/β-CD because of the force of the host–guest recognition between CD and dabcyl. The MNPs/β-CD–DNA/dabcyl were able to reach the electrode surface through external magnetic field. Therefore, the target hybridization event could be transduced into the detection of the electrochemical signal of the Au nanoparticle. The detection limit was down to 9.930×10^{-13} M for complementary HBV DNA sequence. This method could realize one base-mismatched DNA detection and the distinguish rate was 39.73%. Molecular recognition technology improved the specific selection.[42] Meanwhile the non-immobilizing operation has provided convenience for subsequent experiment and DNA detection was realized directly in solution without other treatment. Therefore, the efficiency of the hybridization and the detection sensitivity were greatly improved. Good electronic transfer ability and magnetic separation ability of magnetic Fe_3O_4 nanoparticles has also increased sensitivity for the detection. The proposed electrochemical sensor offered a promise of a convenient method to ultrasensitive recognition of the target DNA. It would be applied in disease diagnosis as well as other research fields.

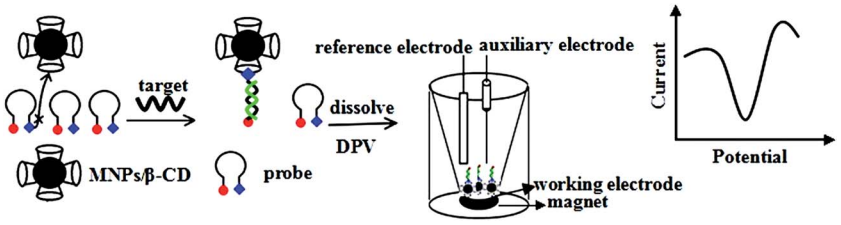

Fig. 1 Schematic representation of electrochemically sensing DNA with hybridization in homogeneous solution *via* host–guest recognition based on the MNPs/β-CD.

2. Experimental

2.1. Apparatus and reagents

Differential pulse voltammetry (DPV) was performed using a CHI Instruments model 420A Electrochemical Analyzer (CHI Instrument Inc., USA). The electrochemical system comprised of a working electrode of glassy carbon electrode, an Ag/AgCl reference electrode and a platinum wire counter electrode. TEM data and energy-dispersive spectroscopy (EDS) spectrum were recorded using a JEM 2100 Transmission Electron Microscope at 200 kV (JEOL, Japan) attached by Energy Disperse Spectroscopy (EDAX, USA). Fourier transform infrared (FT-IR) spectra were obtained on a Nicolet AVATAR 380 FT-IR spectrophotometer (Thermo Fisher Nicolet, USA).

Analytical reagents such as ferric trichloride hexahydrate ($FeCl_3 \cdot 6H_2O$), ethylene glycol ($HOCH_2CH_2OH$), sodium acetate (NaAc), polyethylene glycol ($HO(CH_2CH_2O)_nH$), methacrylic acid ($H_2C{=}C(CH_3)COOH$), acrylamide ($CH_2{=}CHCONH_2$), ethylene glycol dimethacrylate ($CH_2{=}C(CH_3)COOCH_2CH_2OOC(CH_3)C{=}CH_2$) and 2,2′-azobis(2-methylpropionitrile) ($((CH_3)_2C(CN)N{=}NC(CH_3)_2CN$), sodium dihydrogen phosphate (NaH_2PO_4), dipotassium hydrogen phosphate (K_2HPO_4), sodium citrate ($C_6H_5Na_3O_7 \cdot 2H_2O$), ethanol ($C_2H_5OH$), hydrochloric acid (HCl), imidazole, 1-(3-dimethylaminopropyl)-3-ethylcarbodiimide hydrochloride (EDC·HCl), were purchased from Aladdin Reagent Co. Ltd (Shanghai, China). $HAuCl_4$ was purchased from Sinopharm Group Co. Ltd (Shanghai, China). Phosphate-buffered saline (PBS, 0.1000 M, pH 7.0) was prepared with NaH_2PO_4 and K_2HPO_4. Amino-β-cyclodextrin (β-CD-NH_2) was purchased from Binzhou Zhiyuan Bio-Technology Co. Ltd (Shandong, China). Ultrapure water was used from Aquapro system (specific resistance is 13 MΩ cm).

DNA was obtained from Sangon Biotechnology Inc. (Shanghai, China). The hairpin probe DNA sequence was 5′-DABCYL-$(CH_2)_3$-CGT AGG GCC AAC AGC CAG TGG GAA ACC CTG CG-$(CH_2)_6$-SH-3′.

The target DNA sequence was 5′-GTT TCC CAC TGG CTG TTG GC-3′.

One base mismatched sequence was used in the contrasting and selectivity experiments and the sequence was 5′-GTT TCC CAC AGG CTG TTG GC-3′.

Non-complementary DNA sequence was 5′-GCG AGT TTG AGG TGC GTG TTT-3′.

2.2. Preparation of Fe_3O_4 nanoparticles

Fe_3O_4 nanoparticles were prepared according to the literature:[43] $FeCl_3 \cdot 6H_2O$ (0.6826 g, 2.500 mmol) was dissolved in $HOCH_2$-CH_2OH (20.00 mL) to form a clear solution, followed by the addition of NaAc (1.8000 g) and $HO(CH_2CH_2O)_nH$ (0.5000 g). The mixture was stirred vigorously for 30 min and then sealed in an autoclave (35.00 mL capacity). It was heated and maintained at 200 °C for 12 h, and then allowed to cool to room temperature. The black products were washed several times with ethanol and dried at 80 °C for 6 h.

2.3. Carboxylation of magnetic Fe_3O_4 nanoparticles

The carboxyl magnetic Fe_3O_4 nanoparticles were prepared according to the literature.[44] The as prepared magnetic Fe_3O_4 nanoparticles solution (2.00 mL), $H_2C{=}C(CH_3)COOH$ (30.00 mg), $CH_2{=}CHCONH_2$ (30.00 mg), $CH_2{=}C(CH_3)COOCH_2CH_2$-$OOC(CH_3)C{=}CH_2$ (20.00 mg) and $(CH_3)_2C(CN)N{=}NC(CH_3)_2CN$ (25.00 mg) as initiator were dispersed in acetonitrile (40.00 mL) and ultrasonicated for 10 min. Then the mixture was heated to boil for 2 h. During the process, occasional ultrasonication was used to prevent the nanoparticles from aggregation. The obtained nanoparticles were magnetically separated by external magnetic field and washed with C_2H_5OH and H_2O for three times. Then the nanoparticles were dispersed in water (4.00 mL) to form a solution (about 5.00 mg mL^{-1} for Fe_3O_4) and stored for use.

2.4. Preparation of MNPs/β-CD

MNPs/β-CD were prepared according to following processes. Firstly, 50.00 mg β-CD-NH_2 was dissolved into 100.00 mL water to form a clear solution, then 5.00 mL of imidazole (0.5000 M) was added into it. After stirring for 30 minutes, 5.00 mL of EDC·HCl (0.5000 M) and 0.20 mg of MNPs were added to it. The resulting mixture was stirred for 12 h at room temperature and then continued to centrifuge for 30 min at 5500 rpm to remove the excessive β-CD. The precipitate was washed with 0.1000 M PBS three times and redispersed in 0.1000 M PBS. Then, the resulting solution was stored in the refrigerator for further use.

2.5. Preparation of Au nanoparticles

Au nanoparticles were prepared according to the literature.[45] In brief, 100.00 mL of boiling aqueous solution containing 1.00 mL of 1% $HAuCl_4$ solution was brought to reflux with stirring, and 2.50 mL of 1% $C_6H_5Na_3O_7 \cdot 2H_2O$ solution was introduced into this $HAuCl_4$ solution. The mixture solution was kept boiling for another 30 min and left to cool to room temperature. The diameter of the prepared Au nanoparticles were around 10 nm by transmission electron microscopy scanning. The obtained Au nanoparticles were then stored in brown glass bottle at 4 °C for further use.

2.6. Preparation of the probe DNA

Au nanoparticles were mixed with the probe DNA for 16 hours, and the resulting solution was centrifugated for 20 min at 12 000 rpm to remove excess oligonucleotides. The wine red Au/DNA precipitate was washed with 0.1000 M PBS and redispersed in 0.1000 M PBS. The resulting probe solution was stored in the refrigerator for use. Au nanoparticles-labeled probe DNA was identified by UV spectrophotometry.

2.7. DNA hybridization and host–guest recognition

The target DNA was prepared by adding 58 μL PBS (0.1000 M, pH 7.0) into the centrifugal tube to the concentration of 1.003×10^{-4} M DNA solution, then continued to dilute. The assay procedure was initiated by adding 10 μL of the target DNA in the hybridization buffer solution, containing 0.20 mg of MNPs/

β-CD and 10 μL of the probe Au–DNA. 80 μL of PBS was added and the solution was stirred for 80 min at 40 °C to carry out the hybridization reaction. After the incubation, the conjugates were washed with 100 μL of PBS buffer, the supernatant fluid could be discarded through the magnetic separation and non-specifically bound gold nanoparticles could be eliminated.

2.8. Electrochemical detection

All electrochemical experiments were directly performed in an electrochemical cell, with a glassy carbon working electrode (diameter = 5.0 mm) at the bottom, an Ag/AgCl (saturated KCl) reference electrode and a platinum auxiliary electrode. The final MNPs/β-CD–target DNA–probe DNA/Au nanoparticles conjugates were dissolved in 1.00 mL of 0.1000 M HCl solution. Then, +1.25 V was applied for 120 s to carry out the electrochemical preoxidation of Au. Differential pulse voltammetry (DPV) scanning was followed on in the range from +0.65 V to +0.25 V (Incr *E*: 0.004 V; amplitude: 0.05 V; pulse width: 0.05 s; pulse period: 0.2 s). During the potential scanning, a well-resolved electrochemical signal was obtained at the potential around +0.40 V due to the reduction of $AuCl_4$ which was used for the identification and quantification of the target DNA.[23]

3. Results and discussion

3.1. The electrochemical DNA sensing based on the host–guest recognition

To test the feasibility of the assay, contrastive experiments were performed to investigate the electrochemical DNA sensing based on the host–guest recognition. As shown in Fig. 2, curve a, when DNA probe and MNPs/β-CD were incubated in the absence of target DNA according to the procedure, only a relatively small DPV current signal was obtained (a). Contrarily, a marked electrochemical signal was obtained (b) after the target DNA was added. It was demonstrated that before the hybridization, the probe remained the "closed" state and retained the stem-loop structure. Due to the steric effect of Au nanoparticles and the stem-loop structure of probe DNA, the dabcyl was prevented from entering the cavity of the β-CD.[24] Therefore, there was no obvious signal displayed. Once in the presence of the target DNA, the probe was hybridized with the target DNA in a homogeneous solution. They formed into a rigid double-strand hybridization structure, therefore, the dabcyl molecule entered into the cavity of CD based on host–guest recognition. Then, the Au nanoparticles were captured onto the electrode through external magnetic field. Finally, the specific DNA sequence determination was translated into Au-nanoparticle electrochemical signal. The hybridization could be realized in homogeneous solution without immobilizing the probe on the electrode by this method.

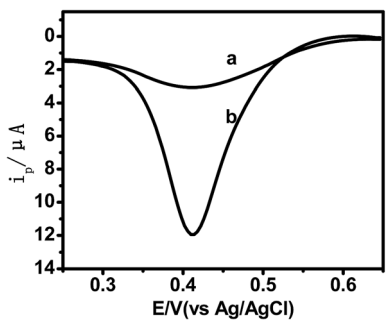

Fig. 2 The DPV responses of the sensor in the absence of target DNA (a) in the presence of 1.505×10^{-11} M target DNA (b). The electrochemical detection was performed when 10 μL of 2.860×10^{-10} M DNA probe and 0.20 mg magnetic MNPs/β-CD were incubated with PBS, then it was dissolved in 0.1000 M HCl solution, immediately after the electrochemical oxidation of Au nanoparticles at +1.25 V for 120 s, DPV was performed with scan range from +0.65 to +0.25 V with pulse amplitude 50 mV and pulse width 50 ms.

3.2. The UV-vis spectra of probe DNA

Au nanoparticle-labeled probe DNA was identified by UV spectrophotometry. It was shown in Fig. S1.† Au nanoparticles appeared to be wine red and had a maximum absorbance at 520 nm.[46] It was found that after DNA was labeled with Au nanoparticles, the characteristic absorption peak of Au nanoparticles didn't change, but the characteristic absorption peak of DNA at 260 nm emerged. It showed that the probe DNA had been labeled with Au nanoparticles.[47] Au nanoparticles were detected as a tag in the following experiments.

3.3. The FT-IR spectra of MNPs/β-CD

MNPs/β-CD was prepared for host and guest recognition in subsequent experiments. The FT-IR spectra of MNPs (a), MNPs-carboxyl (b) and MNPs/β-CD (c) were compared in the range of 400–4000 cm^{-1}. As shown in Fig. S2,† the peak at 580 cm^{-1} was the characteristic absorption of the magnetic nanoparticle, Fe_3O_4. Compared with the magnetic Fe_3O_4, carboxyl-Fe_3O_4 has the vibration absorption of the carboxylic group and the characteristic absorption of the O–H bond is at the broad peak of 3300–3400 cm^{-1}. The intense peak seen at 1086 cm^{-1} corresponding to the coupled ν(C–C/C–O) stretch vibration of MNPs/β-CD (Fig. S2c†). The peak at 1384 cm^{-1} could be attributed to the C–N stretch vibration in the amide bond (–CO–NH–) of MNPs/β-CD (Fig. S2c†), while this peak in the carboxyl-Fe_3O_4 was absent (Fig. S2b†), indicative of surface attachment by formation of an amide bond between the β-CD and carboxyl-Fe_3O_4.[48] Therefore, β-CD was successfully attached to the magnetic Fe_3O_4 nanoparticles.

3.4. The formation of MNPs/β-CD–target DNA–probe DNA/Au conjugates

The morphology and components of MNPs/β-CD–target DNA–probe DNA/Au conjugates were investigated by transmission electron microscopy (TEM) and Electron Dispersive Spectroscopy (EDS) (Fig. S3†). One sample was prepared according to the protocol, in the presence of the target DNA, after the incubation and wash, the sample was diluted by 600 μL distilled water, 30 μL of the resultant solution was used for TEM. Fig. S3a and b† showed that gold nanoparticles adhered on the magnetic nanoparticles. It could be seen from the images that magnetic nanoparticles had an average diameter of around 200 nm. It

dispersed compactly possibly because of the magnetic dipole–dipole attractions.[49] Au nanoparticles had an average diameter of 10 nm, and it looked more light in TEM image.[50] As shown in Fig. S3a and b,† it is interesting to observe that some grey nanoparticles with a size of about 10 nm were coated on the core surface of Fe_3O_4. This has identified that in the presence of the target DNA, the dabcyl molecule could be captured by the MNPs/β-CD through the host–guest recognition. Therefore the conjugates of MNPs/β-CD–target DNA–probe DNA/Au were formed and gold nanoparticles were adhered onto the magnetic nanoparticles. Magnetic nanoparticle and gold nanoparticles appeared to be in a cluster state, for that in the presence of the target DNA, the magnetic nanoparticle might form the network structure through the formation of MNPs/β-CD–target DNA–probe DNA/Au conjugates *via* the host–guest recognition.

The spectrum of electron dispersive spectroscopy (EDS) of the conjugates was conducted and shown in Fig. S3c.† There the peaks of Au, Fe, and O elements present, and the atomic ratio of Fe/O is near 3 : 4, confirmed the successful coating of Au on Fe_3O_4. It coincided well with the TEM results that the gold nanoparticle were adhered onto the magnetic nanoparticle through the host–guest recognition.

3.5. The amount of MNPs/β-CD

The amount of MNPs/β-CD might have an influence on the determination of the target DNA, therefore, it was examined and optimized. As shown in Fig. 3, the DPV responses increased along with the increase of the amount of MNPs/β-CD in the range of 0.04 mg to 0.32 mg. The responses increased up to 0.20 mg and then leveled off. No significant increase was observed when it was over than 0.20 mg. This behavior corresponded to the fact that with an increasing amount of magnetic particles, the surface of the electrode become saturated with the particle, and therefore, 0.20 mg of magnetic MNPs/β-CD was employed in the subsequent work.

3.6. Thermal denaturation tests of the probe DNA

In order to study the effect of the temperature on the stem loop structure, the electrochemical responses of the probe at different temperatures were monitored (Fig. 4). As shown in Fig. 4a, without the target, at lower temperatures, the probe was

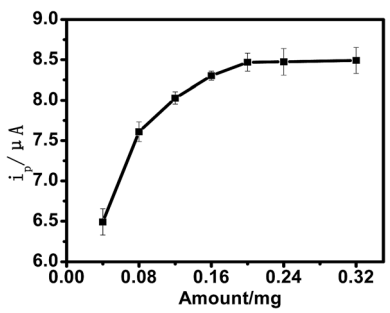

Fig. 3 The amount of MNPs/β-CD with 2.860×10^{-10} M probe and 1.505×10^{-11} M target DNA. Error bars = ±relative standard deviation and $n = 5$.

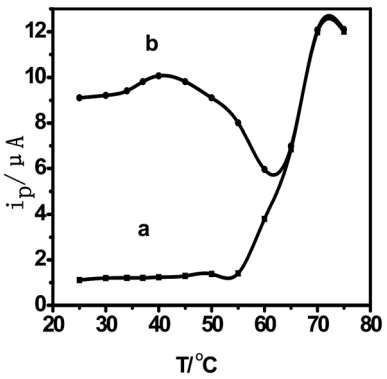

Fig. 4 Thermal denaturation tests of the probe (2.860×10^{-10} M): (a) in the absence of target, (b) in the presence of target (1.505×10^{-11} M).

in a closed stem loop state and kept the hairpin stem. There was only a relatively small DPV current signal. While at high temperatures, the helical order of the stem gave way to a random-coil configuration, restoring electrochemical response. The transition occurred at 61 °C. The obtained melting temperature was consistent with the value of 59 °C predicted (http://dimamelt.bioinfo.rpi.edu). Due to the stem-loop structure, the melting temperature was higher than the linear structure[51] and similar with other stem-loop structure.[52] While in the presence of the target DNA, the response curve at different temperatures (Fig. 4b) showed that the peak current increased as the temperature increased at low temperatures, but as the temperature reached 40 °C, the current diminished significantly. When the temperature was higher than 60 °C, the DPV response increased significantly. These two curves coincide after 60 °C. Its shape was similar to the temperature curve of the reported fluorescence determination of DNA.[53] It was deduced from the experiments that in the range of 25 to 40 °C, the increased DPV response was induces by the specific recognition for target DNA not by the self dissociation of the probe.[54]

3.7. The effect of temperature and time

The sensing was strongly influenced by the experimental conditions, such as time and temperature. Therefore, the time and the temperature for the hybridization and host–guest recognition were firstly examined. As shown in Fig. 5, the DPV response reached the maximum when the hybridization time reached 80 min. It was deduced from the experiments that 80 min would assure the fully dissociation of the stem loop structure and the formation of the MNPs/β-CD–target DNA–probe DNA/Au conjugates. The probable reason why the responses decreased after 80 min was that the larger particles might aggregate after 80 min, which affected the binding affinity between MNPs/β-CD and dabcyl.[55] When the temperature was higher than 40 °C, the response was also decreased, for that higher temperature might cause the denaturation of DNA and result in lower hybridization efficiency.[56] Therefore 80 min and 40 °C were chosen as optimal for the proposed DNA hybridization detection.

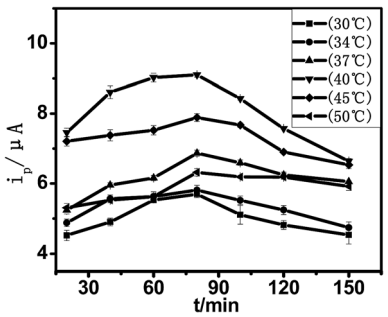

Fig. 5 The effect of temperature and time on the peak current with 2.860×10^{-10} M probe and 1.505×10^{-11} M target DNA. Error bars = ±relative standard deviation and $n = 5$.

3.8. Quantitative analysis of the target DNA

In the experiments, the DNA probe and MNPs/β-CD were incubated with different concentrations of target DNA at 40 °C for 80 min, and then the peak current of the reduction of $AuCl_4^-$ was measured as the hybridization signal. As shown in Fig. 6, one continuously enhancing DPV response was obtained with the concentration of the target DNA sequence increased. The inset displayed the calibration curve of the DPV response of the sensor to the concentration of the target DNA, which presents a linear range from 1.505×10^{-12} to 3.010×10^{-10} M. The equation for the resulting calibration plot was $i_p = 0.2191 + 5.795 \log c$ (c/10^{-12} M) with the correlation coefficient of 0.9966 and the detection limit of 9.930×10^{-13} M. The sensitivity of the biosensor was better than some previous reports, the magnetically trigged direct electrochemical detection of DNA hybridization using Au[67] quantum dot (1.200×10^{-8} M),[57] metal nanoparticle-based electrochemical stripping potentiometric detection of DNA hybridization (1.500×10^{-8} M).[58] The R.S.D. of five replicate determination was 8.163%. It could be found that our sensor displayed improved sensitivity. The high sensitivity of the sensor was attributed to the homogeneous hybridization system and the introduction of the magnetic nanoparticles and Au nanoparticles.

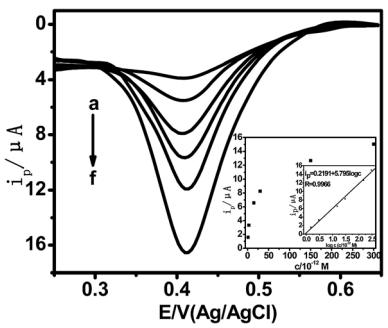

Fig. 6 DPV responses of different concentrations of the target DNA (a) 1.505×10^{-12}, (b) 3.010×10^{-12}, (c) 1.505×10^{-11}, (d) 3.010×10^{-11}, (e) 1.505×10^{-10}, (f) 3.010×10^{-10} M. Inset: the linear plot of the regression equation in the concentration range of 1.505×10^{-12} to 3.010×10^{-10} M. Error bars = ±relative standard deviation and $n = 5$.

3.9. Selectivity of the sensor

The selectivity of the biosensor was evaluated by using probe DNA to hybridize with non-complementary sequences (c), single base mismatched sequences (b) and complete complementary sequences (a) with different concentrations. The resulting plots of the peak current *versus* different DNA sequences were shown in Fig. 7. Significant differences were observed between the complementary target DNA and one-mismatched DNA when the DNA concentration was more than 3.010×10^{-12} M, which was used as the threshold for visually discriminating complementary target DNA and one base-matched DNA. In addition, there was no obvious response observed in the presence of non-complementary DNA, implying that non-complementary DNA would not hybridize with the DNA probe. The ability to distinguish point mutation by this sensor was comparable to that described in the literature.[59] When adding 10 μL of 1.505×10^{-11} M complementary target DNA, the non-complementary DNA produced neglectable DPV signal (N), and the one base-mismatched DNA (M) generated about 39.73% of the DPV response (M) that induced by the fully complementary target DNA (T). The selectivity of this sensing system was higher than the reported signal-on E-DNA senor for electrochemical detection of DNA (63%),[60] a versatile signal-off strategy for fluorescent detection of DNA based on quantum dots (54.3%)[61] and a DNA detection platform based on a combination of hairpin DNA switch, AuNPs and enzyme amplification (40%).[62] It has been reported that molecular beacons behaved well in discriminating single-nucleotide polymorphisms in homogeneous systems. It was due to the fact that the hybridization reaction between the target DNA and the probe should overcome the intrinsic hydrogen bond energy of the molecule beacon's stem part, and the hybridizer molecule should stretch into a straight conformation. Therefore, the high selectivity of the sensor may be attributed to the stem-loop structure of the DNA probe and the intrinsic host–guest recognition strategy.

The determination performance of the sensor for HBV sequences in this work was compared with other methods. From Table 1, it was clear that this strategy showed a lower

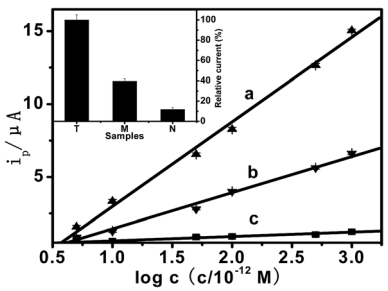

Fig. 7 The calibration plots of peak current of DPV at the concentration in the range of 1.505×10^{-12} M up to 3.010×10^{-10} M: (a) with adding complementary target DNA, (b) with adding one base-mismatched DNA and (c) with adding non-complementary DNA. Error bars = ±relative standard deviation and $n = 5$. Inset: the column diagram of peak current of DPV at the concentration of 3.010×10^{-11} M: (T) complementary target DNA, (M) one base-mismatched DNA and (N) non-complementary DNA.

Table 1 The comparison of determination performance of the sensor with other methods

Method	Linear range (M)	LOD (M)	Selectivity	Ref.
Fluorescence	0 to 5.0×10^{-7}	4.0×10^{-9}	—	63
Electrochemistry	0 to 5.0×10^{-9}	8.5×10^{-11}	—	64
Fluorescence	0.5×10^{-9} to 1.0×10^{-8}	1.48×10^{-10}	—	65
Fluorescence	4.5×10^{-11} to 6.0×10^{-9}	1.5×10^{-11}	About 50%	66
Our sensor	1.505×10^{-12} to 3.010×10^{-10}	9.930×10^{-13}	39.73%	

detection limit, which could be attributed to the non-immobilization strategy, the host–guest recognition and the adoption of the nanoparticles.

4. Conclusions

In summary, a non-immobilizing electrochemical DNA sensing strategy was constructed to allow the hybridization between DNA probe and target DNA in homogeneous solution. The sensor achieved the higher selectivity, sensitivity, simplicity and efficiency for the determination of HBV sequence-specific DNA. Based on the non-immobilizing hybridization system and host–guest recognition technology, the direct modification of the target was avoided and the detection efficiency was greatly improved. In this sensing protocol, the electrochemical responses with the concentration of HBV DNA over a range from 1.505×10^{-12} to 3.010×10^{-10} M were detected and the detection limit obtained was 9.930×10^{-13} M. This sensor provided a more universal method for the assay of disease-related DNA with high selectivity. It would find potential application in genetic studies and disease diagnosis.

Acknowledgements

We would like to express our gratitude to Shanghai Natural Science Foundation (No. 13ZR1418300) and National Natural Science Foundation of China (No. 21275054) for financial support of this work.

References

1 T. R. Golub, D. K. Slonim, P. Tamayo, C. Huard, M. Gaasenbeek, J. P. Mesirov, *et al.*, *Science*, 1999, **286**, 531–537.
2 D. J. Weatherall and A. O. Wilkie, *Curr. Opin. Genet. Dev.*, 1996, **6**, 271–274.
3 M. J. Heller, *Annu. Rev. Biomed. Eng.*, 2002, **4**, 129–153.
4 H. Peng, L. Zhang, T. H. M. Kjallman, C. Soeller and J. Travas-Sejdic, *J. Am. Chem. Soc.*, 2007, **129**, 3048–3049.
5 S. S. Zhang, H. Zhong and C. F. Ding, *Anal. Chem.*, 2008, **80**, 7206–7212.
6 Y. F. Wu, S. Q. Liu and L. He, *Anal. Chem.*, 2009, **81**, 7015–7021.
7 C. Y. Lee, P. C. T. Nguyen, D. W. Grainger, L. J. Gamble and D. G. Castner, *Anal. Chem.*, 2007, **79**, 4390–4400.
8 C. E. Immoos, S. J. Lee and M. W. Grinstaff, *J. Am. Chem. Soc.*, 2004, **126**, 10814–10815.
9 H. Cai, X. N. Cao, Y. Jiang, P. G. He and Y. Z. Fang, *Anal. Bioanal. Chem.*, 2003, **375**, 287–293.
10 F. Jelen, B. Yosypchuk, A. Kourilová, L. Novotný and E. Palecek, *Anal. Chem.*, 2002, **74**, 4788–4793.
11 P. Kara, K. Kerman, D. Ozkan, B. Meric, A. Erdem, Z. Ozkan and M. Ozsoz, *Electrochem. Commun.*, 2002, **4**, 705–709.
12 J. Wang, R. Polsky, A. Merkoci and K. L. Turner, *Langmuir*, 2003, **19**, 989–991.
13 J. Wang, D. Xu, A. Erdem, R. Polsky and M. A. Salazar, *Talanta*, 2002, **56**, 931–938.
14 J. Wang, G. Liu and A. Merkocüi, *J. Am. Chem. Soc.*, 2003, **125**, 3214–3215.
15 R. Subbiah, M. Veerapandian and K. S. Yun, *Curr. Med. Chem.*, 2010, **17**, 4559–4577.
16 J. Wang, D. K. Xu, A. N. Kawde and R. Polsky, *Anal. Chem.*, 2001, **73**, 5576–5581.
17 S. J. Park, T. A. Taton and C. A. Mirkin, *Science*, 2002, **295**, 1503–1506.
18 J. Wang and A. N. Kawde, *Electrochem. Commun.*, 2002, **4**, 349–352.
19 D. J. Maxwell, J. R. Taylor and S. Nie, *J. Am. Chem. Soc.*, 2002, **124**, 9606–9612.
20 J. C. Harper, R. Polsky, D. R. Wheeler, S. M. Dirk and S. M. Brozik, *Langmuir*, 2007, **23**, 8285–8287.
21 J. Zhang, R. J. Lao, S. P. Song, Z. Y. Yan and C. H. Fan, *Anal. Chem.*, 2008, **80**, 9029–9033.
22 F. Xuan, X. T. Luo and I. M. Hsing, *Anal. Chem.*, 2012, **84**, 5216–5220.
23 H. F. Cui, L. Cheng, J. Zhang, R. H. Liu, C. Zhang and H. Fan, *Biosens. Bioelectron.*, 2014, **56**, 124–128.
24 H. Fan, Y. Xu, Z. Chang, R. Xing, Q. J. Wang, P. G. He and Y. Z. Fang, *Biosens. Bioelectron.*, 2011, **26**, 2655–2659.
25 B. A. Du, Z. P. Li and C. H. Liu, *Angew. Chem., Int. Ed.*, 2006, **45**, 8022–8025.
26 J. J. Storhoff, A. D. Lucas, V. Garimella, Y. P. Bao and U. R. Müller, *Nat. Biotechnol.*, 2004, **22**, 883–887.
27 I. Yoshimura, Y. Miyahara, N. Kasagi, H. Yamane, A. Ojida and I. Hamachi, *J. Am. Chem. Soc.*, 2004, **126**, 12204–12205.
28 T. Ihara, A. Uemura, A. Futamura, M. Shimizu, N. Baba, S. Nishizawa, N. Teramae and A. Jyo, *J. Am. Chem. Soc.*, 2009, **131**, 1386–1387.
29 J. C. Yan and S. J. Dong, *Electroanalysis*, 1997, **9**, 1219–1222.
30 M. A. Deryabina, S. H. Hansen, J. Østergaard and H. Jensen, *J. Phys. Chem. B*, 2009, **113**, 7263–7269.

31 L. Z. Yang, Y. Xu, X. H. Wang, J. Zhu, R. Y. Zhang, P. G. He and Y. Z. Fang, *Anal. Chim. Acta*, 2011, **689**, 39–46.
32 P. A. Cane, P. Cook, D. Ratcliffe, D. Mutimer and D. Pillay, *Antimicrob. Agents Chemother.*, 1999, **43**, 1600–1608.
33 X. Wang, X. H. Lou, Y. Wang, Q. C. Guo, Z. Fang, X. H. Zhong, H. J. Mao, Q. H. Jin, L. Wu, H. Zhao and J. L. Zhao, *Biosens. Bioelectron.*, 2010, **25**, 1934–1940.
34 T. Sasaki, T. Tahira, A. Suzuki, K. Higasa, Y. Kukita, S. Basa and K. Hayashi, *Am. J. Hum. Genet.*, 2001, **68**, 214–218.
35 J. Wolford, D. Blunt, C. Ballecer and M. Prochazka, *Hum. Genet.*, 2000, **107**, 483–487.
36 M. Li, S. K. Cushing, H. Liang, S. Suri, D. L. Ma and N. Q. Wu, *Anal. Chem.*, 2013, **85**, 2072–2078.
37 M. I. Allen, J. Gauthier, M. DesLauriers, E. J. Bourne, K. M. Carrick, F. Baldanti, L. L. Ross, M. W. Lutz and L. D. Condreay, *J. Clin. Microbiol.*, 1999, **37**, 3338–3347.
38 H. F. Geng, B. Hua, H. Wang, Y. H. Cao, Y. Sun and A. R. Yu, *J. Virol. Methods*, 2006, **132**, 25–31.
39 F. Wightman, T. Walters, A. Ayres, S. Bowden, A. Bartholomeusz, D. Lau, S. Locarnini and S. R. Lewin, *J. Clin. Microbiol.*, 2004, **42**, 3809–3812.
40 A. Bertoletti and A. Gehring, *Expert Rev. Gastroenterol. Hepatol.*, 2009, **3**, 561–569.
41 A. Tsourkas, M. A. Behlke, S. D. Rose and G. Bao, *Nucleic Acids Res.*, 2003, **31**, 1319–1330.
42 Y. Maeda, T. Fukuda, H. Yamamoto and H. Kitano, *Langmuir*, 1997, **13**, 4187–4189.
43 H. Deng, X. L. Li, Q. Peng, X. Wang, J. P. Chen and Y. D. Li, *Angew. Chem., Int. Ed.*, 2005, **117**, 2842–2845.
44 L. Y. Wang, J. W. Bai, Y. J. Li and Y. Huang, *Angew. Chem., Int. Ed.*, 2008, **47**, 2439–2442.
45 A. Doron, E. Katz and I. Willner, *Langmuir*, 1995, **11**, 1313–1317.
46 S. Link and M. A. EI-Sayed, *J. Phys. Chem. B*, 1999, **103**, 4212–4217.
47 H. C. Wei, Q. Y. Ca, R. Rahn, X. S. Zhang, Y. Wang and M. Lebwohl, *Biochemistry*, 1998, **37**, 6485–6490.
48 J. Pinson and F. Podvorica, *Chem. Soc. Rev.*, 2005, **34**, 429–439.
49 Y. Lalatonne, J. Richardi and M. P. Pileni, *Nat. Mater.*, 2004, **3**, 121–125.
50 J. Zheng, L. Li, G. F. Cheng, A. B. Wang, X. L. Tan, P. G. He and Y. Z. Fang, *Sci. China, Ser. B: Chem.*, 2007, **50**, 351–357.
51 J. H. Oh and J. S. Lee, *Anal. Chem.*, 2011, **83**, 7364–7370.
52 C. B. Hughesman, R. F. Turner and C. A. Haynes, *Biochemistry*, 2011, **50**, 5354–5368.
53 G. Bonnet, S. Tyagi, A. Libchaber and F. R. Kramer, *Proc. Natl. Acad. Sci. U. S. A.*, 1999, **96**, 6171–6176.
54 J. Zheng, G. F. Cheng, P. G. He and Y. Z. Fang, *Talanta*, 2010, **80**, 1868–1872.
55 K. G. Stamplecoskie, J. C. Scaiano, V. S. Tiwari and H. Anis, *J. Phys. Chem. C*, 2011, **115**, 1403–1409.
56 G. F. Cheng, J. Zhao, Y. H. Tu, P. G. He and Y. Z. Fang, *Anal. Chim. Acta*, 2005, **533**, 11–16.
57 M. Pumera, M. T. Castaneda, M. I. Pividori, R. Eritja, A. Merkoçi and S. Alegret, *Langmuir*, 2005, **21**, 9625–9629.
58 J. Wang, D. K. Xu, A. N. Kawde and R. Polsky, *Anal. Chem.*, 2001, **73**, 5576–5581.
59 C. A. Marquette, M. F. Lawrence and L. J. Blum, *Anal. Chem.*, 2006, **78**, 959–964.
60 L. P. Qiu, L. Qiu, Z. S. Wu, G. L. Shen and R. Q. Yu, *Anal. Chem.*, 2013, **85**, 8225–8231.
61 S. Su, J. W. Fan, B. Xue, L. H. Yuwen, X. F. Liu, D. Pan, C. H Fan and L. H. Wang, *ACS Appl. Mater. Interfaces*, 2014, **6**, 1152–1157.
62 Y. Y. Zhang, Z. W. Tang, J. Wang, H. Wu, A. H. Maham and Y. H. Lin, *Anal. Chem.*, 2010, **82**, 6440–6446.
63 X. Wang, X. Lou, Y. Wang, Q. C. Guo, Z. Fang, X. H. Zhong, H. J. Mao, Q. H. Jin, L. Wu, H. Zhao and J. L. Zhao, *Biosens. Bioelectron.*, 2010, **25**, 1934–1940.
64 X. Li, K. Scida and R. M. Crooks, *Anal. Chem.*, 2015, **87**, 9009–9015.
65 J. Hu, C. Y. Wen, Z. L. Zhang, M. Xie, J. Hu, M. Wu and D. W. Pang, *Anal. Chem.*, 2013, **85**, 11929–11935.
66 X. C. Lu, X. Dong, K. Y. Zhang, X. W. Han, X. Fang and Y. Z. Zhang, *Analyst*, 2013, **138**, 642–650.

